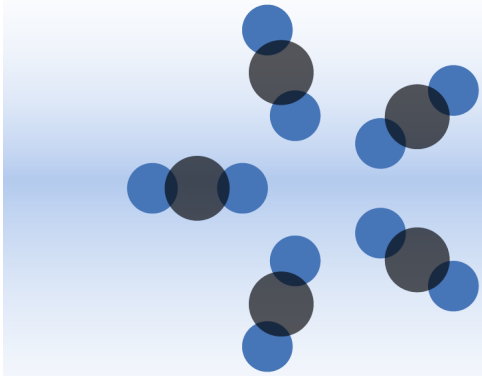

CCSI™

Carbon Capture Simulation Initiative

Steady State and Dynamic MEA Test Runs Conducted in National Carbon Capture Center

November 25, 2014

NETL

Los Alamos NATIONAL LABORATORY EST.1943

Pacific Northwest NATIONAL LABORATORY

BERKELEY LAB

Lawrence Livermore National Laboratory
Science in the National Interest

U.S. DEPARTMENT OF ENERGY

Table of Contents

List of Figures

List of Tables

1. INTRODUCTION

US DOE's Carbon Capture Simulation Initiative (CCSI) has strong focus on developing state of the art, validated models that will ultimately enable new processes to be developed and scaled up more rapidly with lower risk and cost. High quality validation data from large-scale pilot plants for CO_2 capture are rare, and data under dynamic conditions with actual flue gas are not available. With this motivation, members of the CCSI Technical Team recently collaborated with the personnel at the U.S. DOE's National Carbon Capture Center in Wilsonville, AL to obtain high quality data from its pilot scale CO_2 capture process under real operating conditions for MEA-based CO_2 capture systems. The data collected in this test run will enable the development and validation of a "gold standard" solvent model that will serve as a definitive reference for benchmarking the performance of solvent-based CO_2 capture systems. While most of the test runs reported in the literature are steady-state and has focused on narrow operating range, the operating conditions in these test runs were varied widely. In addition, dynamic test runs were conducted by introducing carefully-designed step changes and recording the transients of all key variables. The dynamic test runs were conducted by ensuring that the persistence of excitation of the process is maintained and provides information about the entire spectrum of data with both high and low frequency information (relates to the mechanisms with very short and long time constants). While validating the process model with the dynamic data, the entire temporal profile of all key variables needs to be compared instead of comparing with the single point data collected under steady-state conditions. This will be very useful in identifying model-form and parametric uncertainties in this highly nonlinear electrolyte system. It can be noted that steady-state and dynamic uncertainty quantification (UQ) are two focus areas of CCSI. The test runs conducted at NCCC will enable, for the first time, both steady-state and dynamic UQ using pilot-scale data.

Seventeen steady-state test runs were conducted between 6/2/14 and 6/12/14, Due to blower problems, the test runs were suspended. Again, test runs were resumed on 8/20/14 starting with the dynamic test runs. Finally 6 more steady-state test runs were conducted. The test run concluded on 8/25/14.

2. GENERAL METHODOLOGY: STEADY-STATE AND DYNAMIC TESTS AND MEASUREMENTS

2.1. Steady-State Test Runs

A number of important inputs, disturbances and operating conditions were selected for the steady-state test cases, which include the following variables.

- Solvent flowrate
- Flue gas flowrate
- Flue gas composition
- Lean loading
- Number of beds
- Presence/absence of intercooler

As an example, Figure 1 and Figure 2 show the variation in the inlet gas flow and solvent flow for each value of the reboiler steam flow.

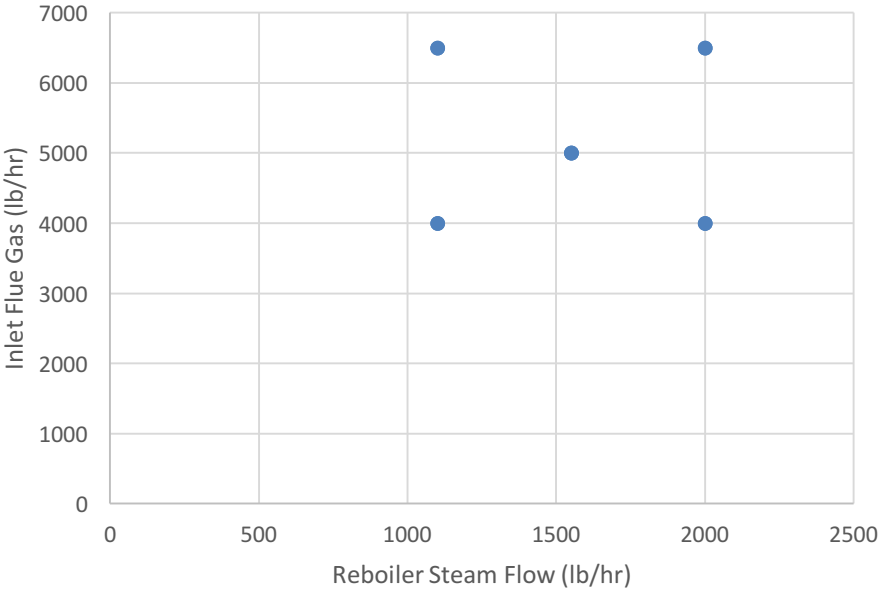

Figure 1: Test matrix for inlet flue gas and reboiler steam flow

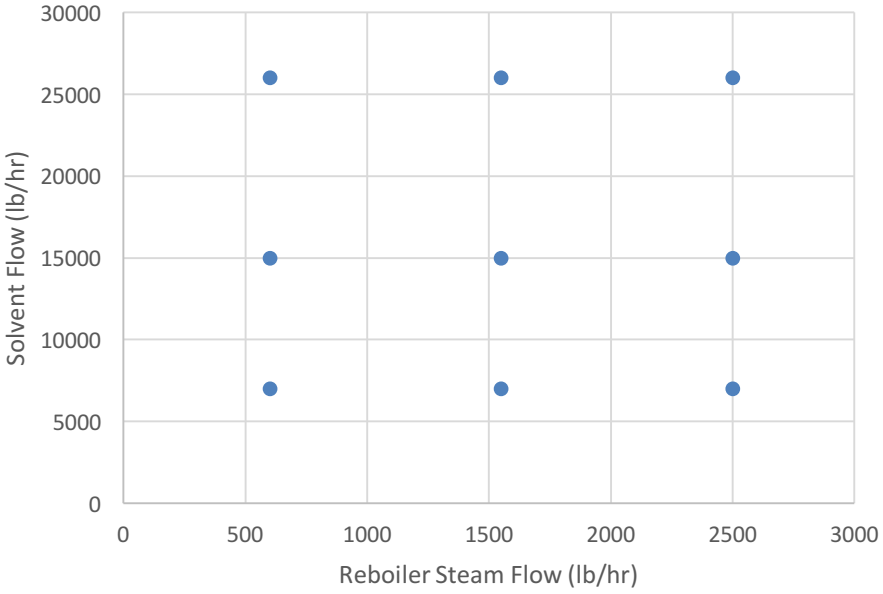

Figure 2: Test matrix for inlet solvent and reboiler steam flow

A set of 31 test runs as shown in Table 1 was proposed. Out of these, 23 test runs were conducted.

Table 1: Steady-state test conducted in the NCCC plant

Test #	Solvent Flow (lb/hr)	Inlet Flue Gas (lb/hr)	Reboiler Steam Flow (lb/hr)	Inlet FG CO2 vol%	# of beds	Inter-cooler
1	15000	5000	1550	10	3	Yes
2	26000	5000	1550	10	3	Yes
3	7000	5000	1550	10	3	Yes
4	15000	5000	600	10	3	Yes
5	15000	5000	2500	10	3	Yes
6	26000	5000	600	10	3	Yes
7	26000	5000	2500	10	3	Yes
8	7000	5000	600	10	3	Yes
9	7000	5000	2500	10	3	Yes
10	15000	5000	1550	11	3	Yes
11	15000	5000	1550	9	3	Yes
12	15000	5000	1550	10	3	No
13	19500	6500	1550	10	3	Yes
14	9100	6500	1550	10	3	Yes
15	15000	5000	1550	10	2	Yes
16	15000	5000	1550	10	2	No
17	15000	5000	1550	10	1	-
18	15000	5000	1550	11	1	-
19	7000	5000	1550	10	1	-
20	26000	5000	1550	10	1	-
21	15000	4000	1100	10	3	Yes
22	15000	6500	1100	10	3	Yes
23	15000	4000	2000	10	3	Yes

24	15000	6500	2000	10	3	Yes
25	15000	4000	1100	10	1	-
26	15000	6500	1100	10	1	-
27	15000	4000	2000	10	1	-
28	15000	6500	2000	10	1	-
29	15000	5000	1550	9	1	-
30	15000	5000	1550	4.5	1	-
31	15000	5000	1550	10	3	No

2.2. Dynamic Test Runs:

As mentioned before, during the dynamic test runs, the focus was on exciting the process so that all its frequencies can be observed. This reflects the underlying nonlinearity of the process. For a nonlinear process it matters whether the step is x or $2x$ since the output will not linearly scale up. In addition, it also matters under what conditions, the step is introduced and whether it is a step increase or decrease. Each successive step is introduced before the process has reached steady-state. Typical set up of dynamic step tests is shown in Table 2.

Table 2: Example set of dynamic step tests in a given input or disturbance

Test#	Test Condition
1	Datum
2	+x% of datum
3	-x% of datum
4	+2x% of datum
5	-2x% of datum
6	+x% of datum
7	-x% of datum
8	Datum

For the NCCC plant, the important inputs and disturbances that are varied are the solvent flow, inlet flue gas, and reoboiler steam flow. Dynamic test strategy for the NCCC plant are shown in Table 3.

Table 3: Dynamic step tests that were completed in the NCCC plant

Test#	Solvent Flow (lb/hr)	Comment
1	12500	Datum
2	13250	value of x_1=750 lb/hr
3	11750	this step results in $2x_1$% decrease from the existing state
4	14000	this step results in $3x_1$% increase from the existing state
5	11000	this step results in $4x_1$% decrease from the existing state
6	13250	this step results in $3x_1$% increase from the existing state, note that even the final value is same as dynamic Test#2, the magnitude is different
7	11750	this step results in $2x_1$% decrease from the existing state, same as test#3, but introduced at different state of excitation
8	12500	return to datum, but doesn't need to settle to datum, next step introduced while the process is through transient
Test#	**Inlet Flue Gas (lb/hr)**	**Comment**
9	5500	value of x_2=500 lb/hr of flue gas
10	4500	this step results in $2x_2$% decrease from the existing state
11	6000	this step results in $3x_2$% increase from the existing state
12	4000	this step results in $4x_2$% decrease from the existing state
13	5500	this step results in $3x_2$% increase from the existing state, note that even the final value is same as dynamic Test#9, the magnitude is different
14	4500	this step results in $2x_2$% decrease from the existing state, same as test#10, but introduced at different state of excitation
15	5000	return to datum

Test#	Reboiler Steam Flow (lb/hr)	Comment
16	1600	value of x_3=500 lb/hr
17	1000	this step results in 2x_3% decrease from the existing state
18	1900	this step results in 3x_3% increase from the existing state
19	700	this step results in 4x_3% decrease from the existing state
20	1600	this step results in 3x_3% increase from the existing state, note that even the final value is same as dynamic Test#16, the magnitude is different
21	1000	this step results in 2x_3% decrease from the existing state, same as test#17, but introduced at different state of excitation
22	1300	return to datum, but doesn't need to settle to datum, next step introduced while the process is through transient
23	1000	return to datum, but for 45 min test
24	1300	value of x=300 lb/hr for steam flow
25	700	this step results in 2x_4% decrease from the existing state
26	1000	return to datum

During the dynamic test runs, a number of issues were accounted for. Typically, the lean solvent samples are sampled after the holding tank, TK20401, which can cause a large damping of the dynamics of the plant, especially the regenerator dynamics may be difficult to observe. This was corrected by manually sampling the lean solvent at the bottom of the regenerator, prior to the stream entering the holding tank. These liquid samples required individual analysis to determine the CO_2 and amine concentrations. The presence of the holding tank, along with a recycle stream, resulted in slower dynamics of the integrated absorber-stripper process while the stripper responded much faster. To accurately observe the dynamics of the stripper as well as the integrated system, separate dynamic tests with shorter and longer time periods between introduction of step changes in the reboiler steam flow rate were conducted.

2.3. Measurements and sensors:

The sensors selected to give data of pressure, temperature, flowrate, composition, density, and viscosity are shown in Table 4. For the absorber, these are able to provide information of the solvent in the column inlet and outlet its temperature and pressure profile and also of the flue gas inlet. Other important data provided by the sensors are the flowrate, temperature and pressure of the solvent returning from the intercoolers. These sensors are highlighted in the flowsheet presented in Figure 3.

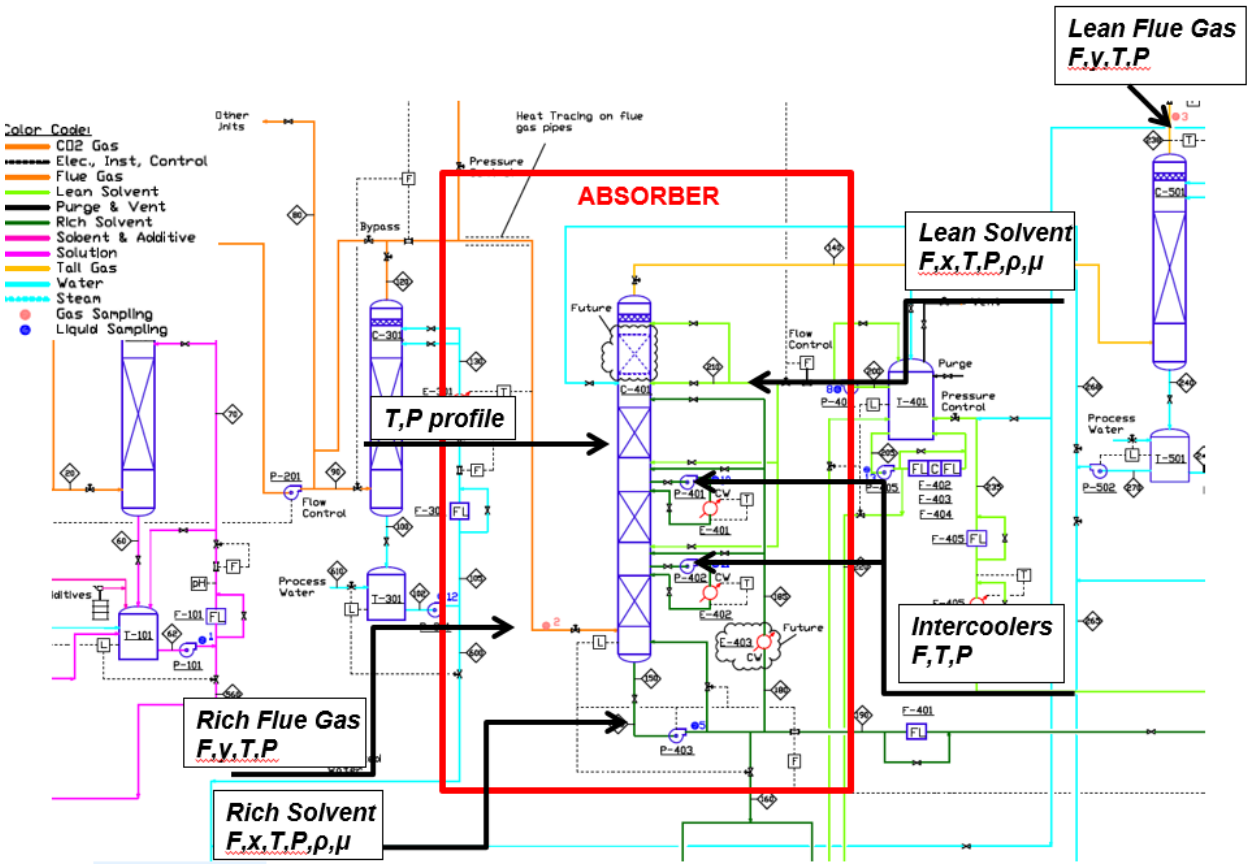

Figure 3: Selected sensors for the absorber

For the regenerator, the sensors were selected to provide information of the rich solvent and of the stripped CO_2 stripped CO_2 (flowrate, composition, density, viscosity, temperature and pressure), also the lean solvent flowrate, solvent flowrate, composition and temperate, as well as the column temperature and pressure profiles. The location of profiles. The location of these sensors is highlighted in the flowsheet presented in

Figure 4.

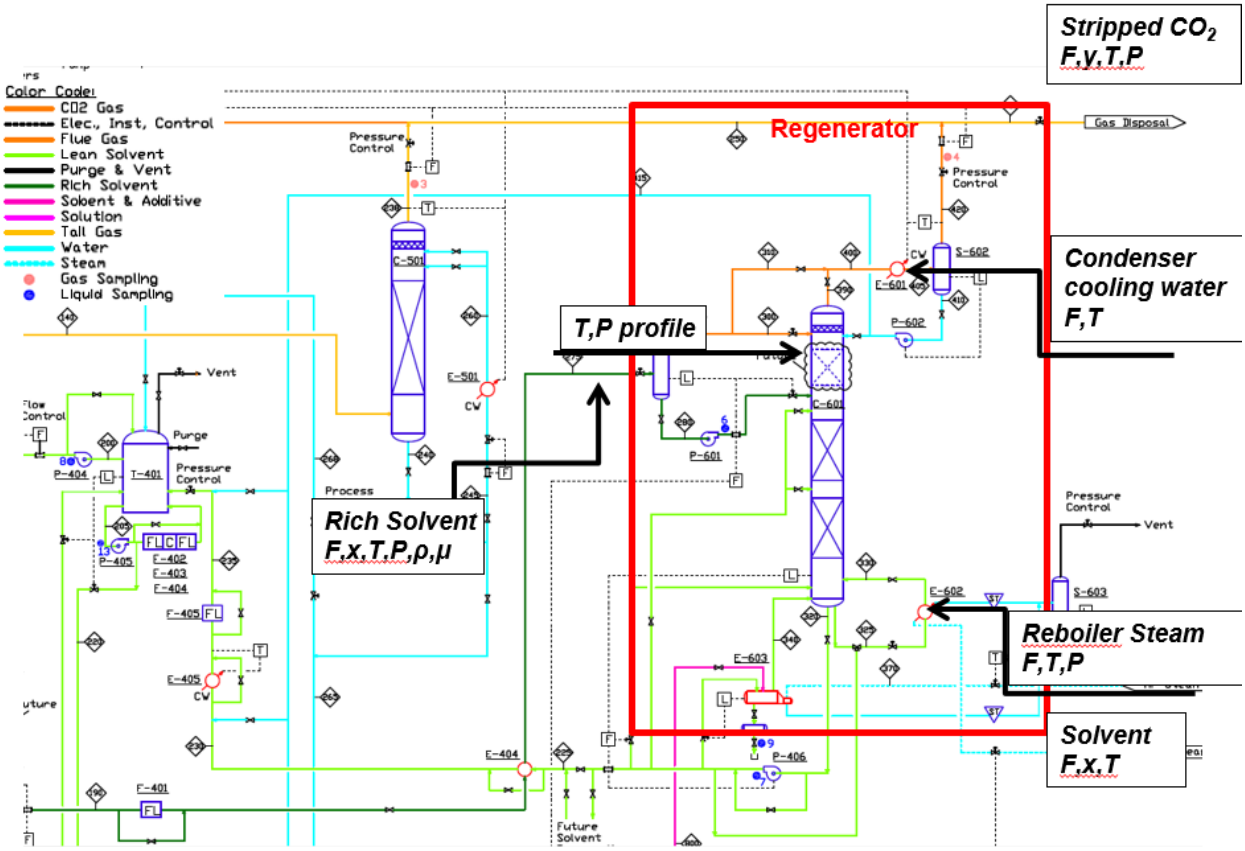

Figure 4: Selected sensors for the regenerator

Table 4: Selected Sensors

Absorber	
Tag	**Description**
TI20101	Temperature indicator at bottom of column
TI20117A-L	Temperature profile in column
TI20119E-F,I-L	Temperature profile in column
PDI20110,PDI20108, PDI20106,PI20101	Pressure profile in column
FI20134,FI20109,F120107	Lean solvent inlet flowrate and composition Rich solvent outlet flowrate and composition Both Intercooler Flowrates (flow through P-401 and P-402) Both Intercooler Return Temperatures (E-401 and E-402 exit temperatures)
TI20112	Lean solvent inlet temperature Lean solvent inlet pressure

TI20102	Rich solvent outlet temperature
PI20100	Rich solvent outlet pressure
	Flue gas inlet flowrate and composition
	Flue gas inlet temperature
	Flue gas inlet pressure
	Flue gas outlet flowrate and composition
TI20115	Flue gas outlet temperature
	Flue gas outlet pressure
	Number of beds in use
	Make-up solvent from T-401
	Inlet Lean Solvent Temperature
	Outlet Lean Solvent Temperature
	Inlet Rich Solvent Temperature
	Outlet Rich Solvent Temperature
	Rich Solvent Pressure Drop
	Lean Solvent Pressure Drop
Regenerator	
TI20221	Temperature indicator at bottom of column
TI20208A-H	Temperature indicators in column packing
TI20230	S-601 Operating Temperature
PI20230	S-601 Operating Pressure
FI20233	Rich solvent inlet flowrate and composition
TI20233	Rich solvent inlet temperature
PI20228	Rich solvent inlet pressure
PDI20209,PDI20210	Pressure profile in column
	Skin temperature in couple of places especially at the reboiler and the bottom sections
	Condenser E-601 duty
	Reboiler steam pressure
	Reboiler steam temperature
	Reboiler steam flowrate
	Lean solvent outlet flow
	Lean solvent outlet temperature
	Lean solvent outlet pressure
	P-406 Outlet Pressure
	S-602 top and bottom flowrates and compositions

3. PRELIMINARY RESULTS

3.1. Viscosity and Density Validation

The viscosity and density data have been compared to the deterministic models for these properties. For viscosity, the model used is given by the equation

$$\mu_{sln} = \mu_{H_2O} \exp\left(\frac{((aW_{MEA}+b)T+cW_{MEA}+d)(\alpha(eW_{MEA}+fT+g)+1)W_{MEA}}{T^2}\right) \quad (1)$$

where temperature is given in Kelvin, α is CO_2 loading (mol CO_2/mol MEA) and W_{MEA} is the weight percent of MEA in solution on a CO_2-free basis. The parameters used in the viscosity equation are given in Table 5.

Table 5: Viscosity parameters

Parameter	Regressed Value
A	-0.0838
B	2.8817
C	33.651
D	1817
E	0.00847
F	0.0103
G	-2.389

The measured values of viscosity are compared to the model predictions, separately for lean solvent and rich solvent, in Figure 5 and Figure 6. Average percent errors for lean and rich solvents are 13.43% and 15.28%, respectively.

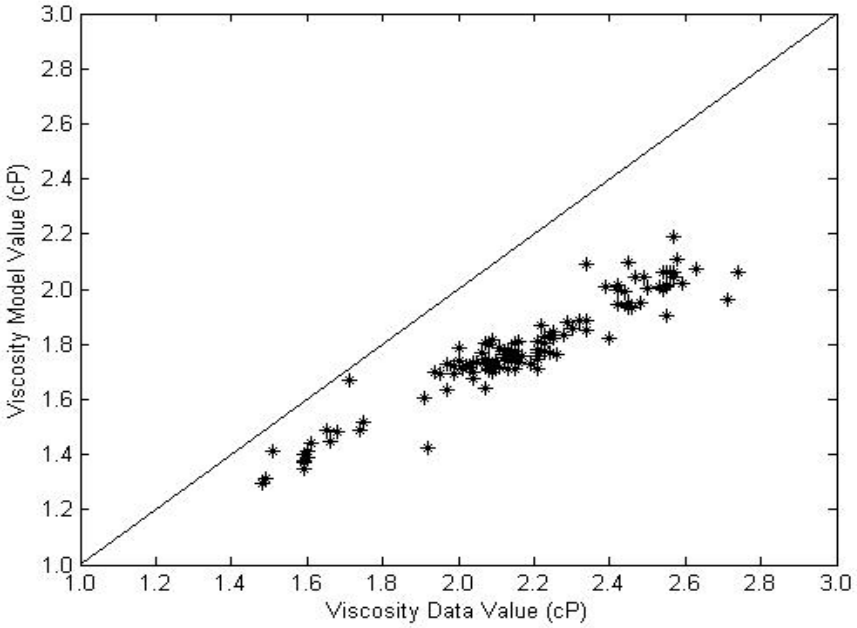

Figure 5: Comparison of data and model viscosity values for lean loading conditions.

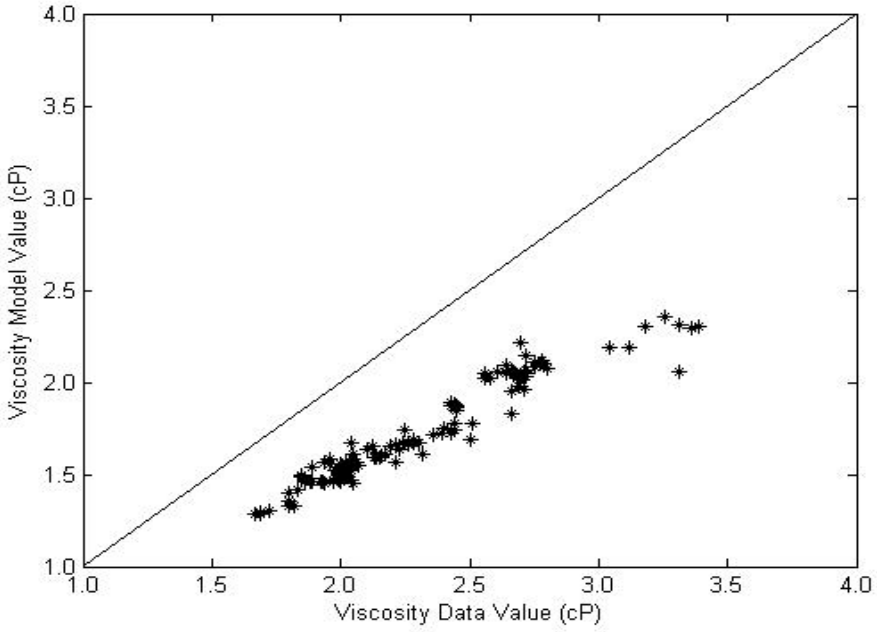

Figure 6: Comparison of data and model viscosity values for rich loading conditions.

As shown in Figure 5 and Figure 6, the model generally underpredicts the viscosity values with respect to the data.

The molar volume model is given by:

$$V_{sln} = X_{MEA}V_{MEA} + X_{H_2O}V_{H_2O} + aX_{CO_2} + (b + cX_{MEA})X_{MEA}X_{H_2O} + (d + eX_{MEA})X_{MEA}X_{CO_2} \quad (2)$$

where the terms given by X_i are apparent species mole fractions, which may be calculated given the solution loading and MEA weight percentage as:

$$X_{MEA} = \left(1 + \alpha + \left(\frac{MW_{MEA}}{MW_{H_2O}}\right)\left(\frac{100}{W_{MEA}} - 1\right)\right)^{-1} \quad (3)$$

$$X_{CO_2} = \alpha X_{MEA}$$

$$X_{H_2O} = 1 - X_{MEA} - X_{CO_2}$$

The pure component molar volumes of water and amine are given as functions of temperature (in Kelvin):

$$V_{H_2O} = \frac{18.1528}{(-3.2484\times10^{-6})T^2 + 0.00165T + 0.793} \quad (4)$$

$$V_{MEA} = \frac{61.08308}{(-5.35162\times10^{-7})T^2 + (-4.51417\times10^{-4})T + 1.19451} \quad (5)$$

The model parameters are given in Table 6.

Table 6: Molar volume parameters

Parameter	Regressed Value
A	10.2074
B	-2.2642
C	3.0059
D	207
E	-563.3701

The data values of density are compared to the model predictions, separately for lean solvent and rich solvent, in Figure 7 and Figure 8.

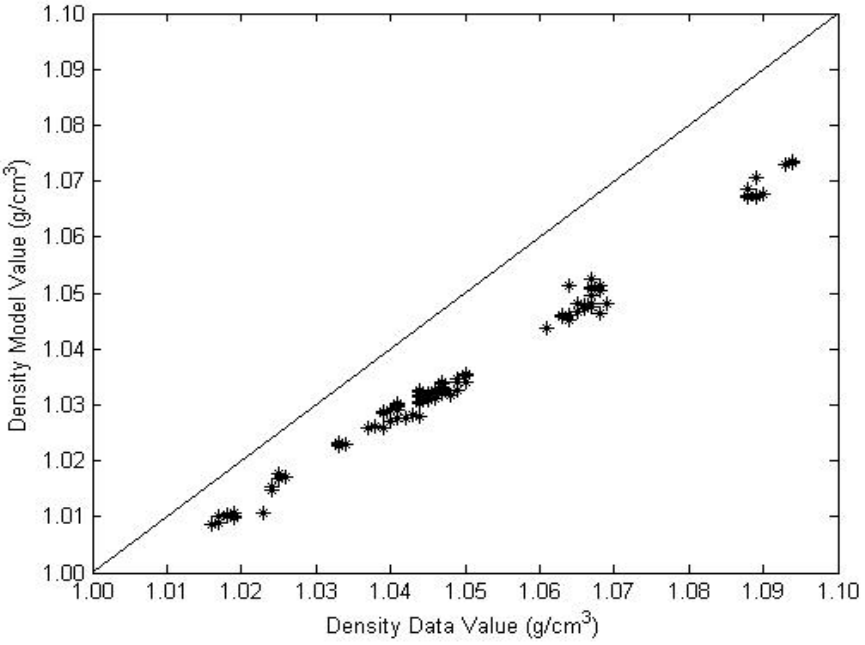

Figure 7: Comparison of data and model density values for lean loading conditions.

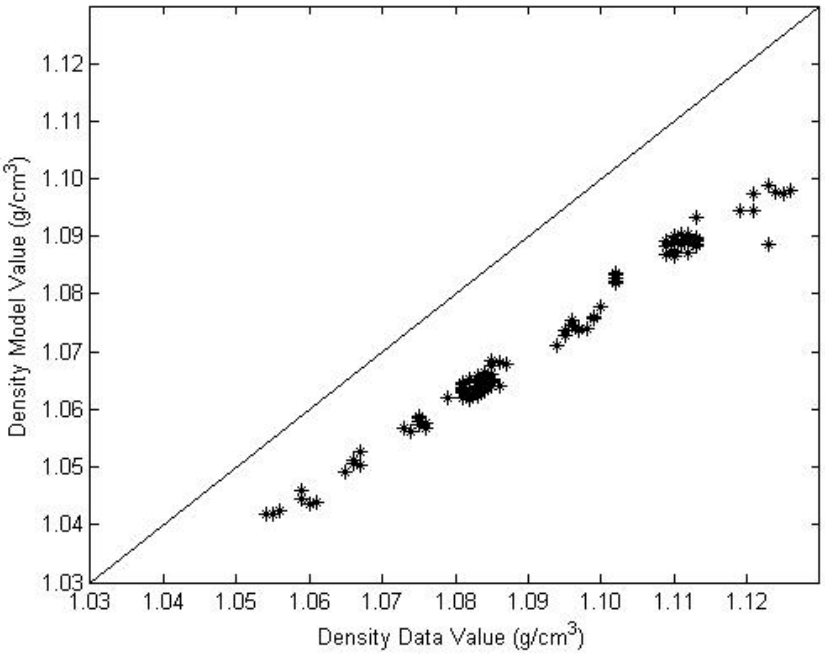

Figure 8: Comparison of data and model density values for rich loading conditions.

As shown in Figure and Figure , the data density values are generally higher than their respective model predictions, which is the same trend shown for the viscosity data. The error given by the model is lower for the density than for the viscosity.

3.2. Steady-State Validations

Some preliminary comparisons of the steady-state data to our deterministic model predictions have been made, separately for the absorber model and the regenerator model. A total of seventeen cases were simulated, and a sample of six of these are presented here. For the absorber model, the major input of interest is the liquid to gas mass ratio. For the regenerator model, the major inputs of interest are the rich solvent flow and the reboiler duty. These inputs are given in Table 7.

Table 7: Inputs for steady-state absorber and regenerator simulations

Case	L:G Mass Ratio	Rich Solvent Flow (kg/hr)	Reboiler Duty (kW)
K1	3.00	7242	434
K3	1.41	3335	431
K4	1.41	3343	431
K9	1.41	3337	167
K11	3.02	7241	429
K16	1.41	4347	423

For the absorber model, the output variables that were used to compare the data to the model predictions were the percent CO_2 capture and the temperature of the outlet rich solvent stream. Percent CO_2 capture is defined as:

$$\%CO_2\ capture = 100 * \left(1 - \frac{\dot{m}_{CO_2,outlet\ flue\ gas}}{\dot{m}_{CO_2,inlet\ flue\ gas}}\right)$$

The comparisons are given in Figure 9 and Figure 10, respectively.

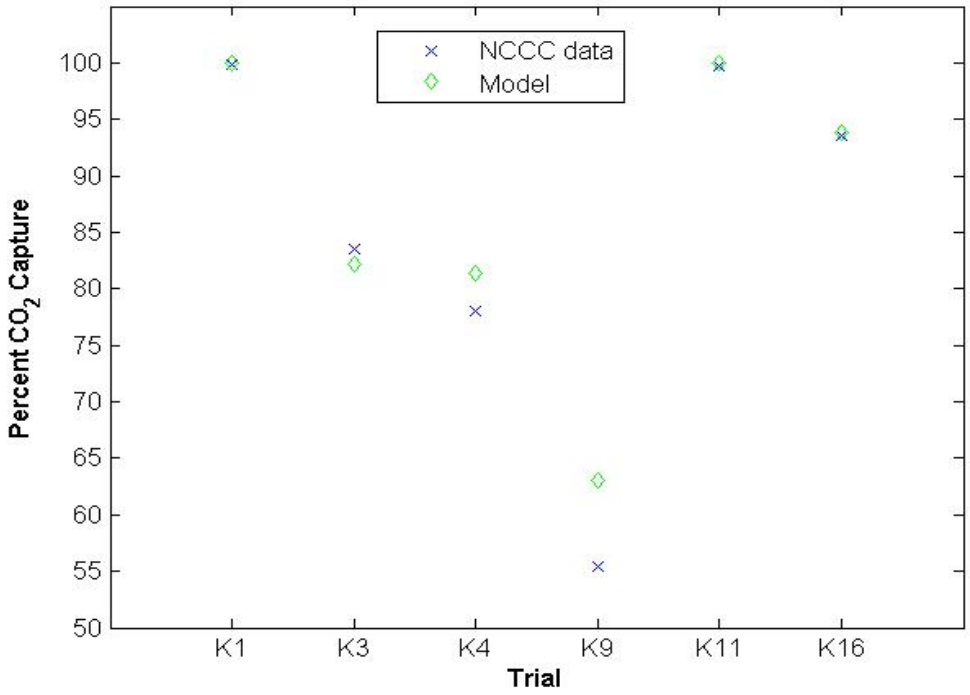

Figure 9: Comparison of model prediction and data for percent CO_2 capture in absorber simulation

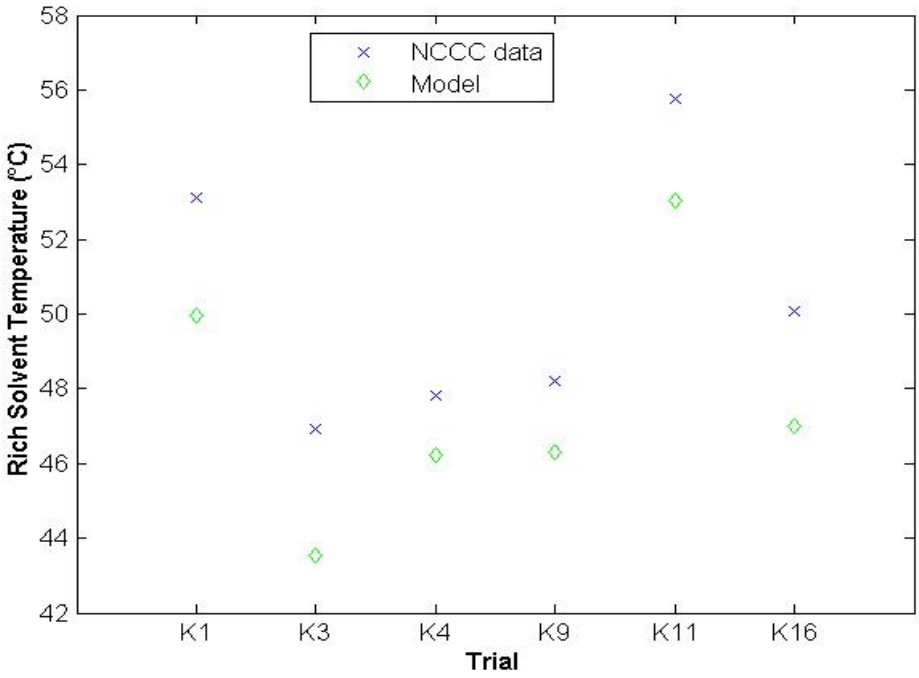

Figure 10: Comparison of model prediction and data for temperature of rich solvent in absorber outlet

As shown in Figure 9, the model predictions match the percent CO_2 capture data relatively well when CO_2 capture percentage remains high. As shown in Figure 10, the model generally underpredicts the temperature of the rich solvent stream in the absorber outlet. This model is still preliminary, and this discrepancy may be due to inaccurate characterization of the heat of absorption of the MEA-H_2O-CO_2 system. It should be noted that in the original Phoenix model, the heat of absorption data were not accounted for while developing the VLE model. This work is currently in progress in CCSI.

For the stripper model, the output variables of interest are the CO_2 loading and temperature of the outlet lean solvent. The comparisons are given in Figure 11 and Figure 12, respectively.

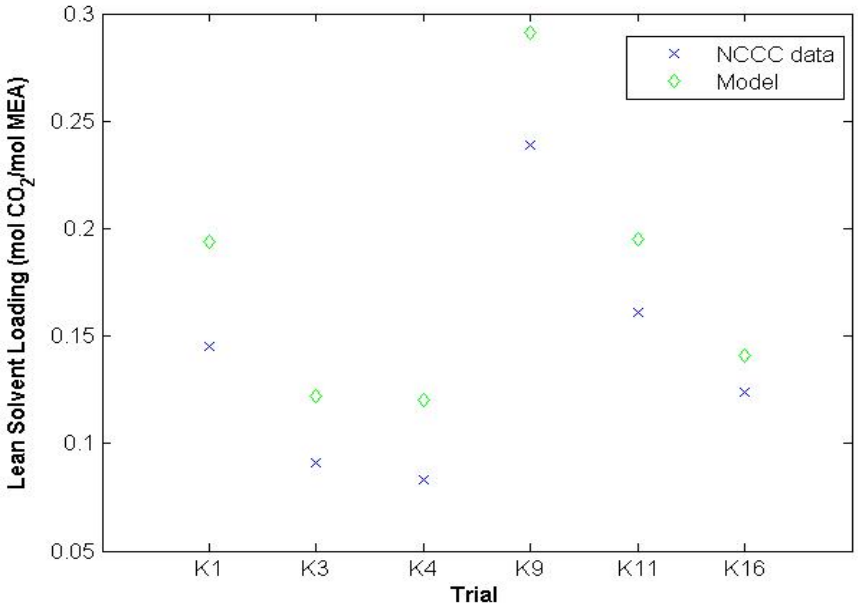

Figure 11: Comparison of model prediction and data for CO_2 loading of lean solvent in stripper outlet

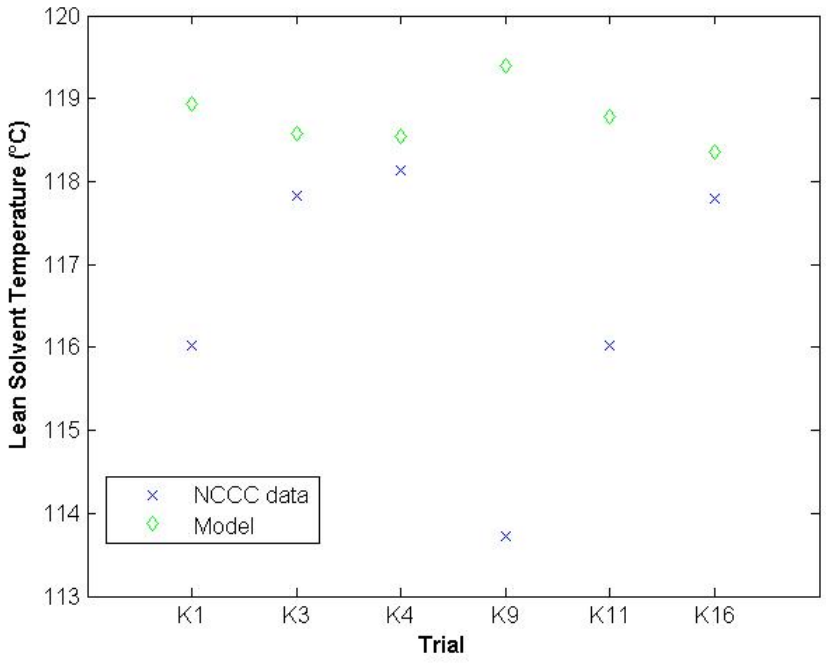

Figure 12: Comparison of model prediction and data for temperature of lean solvent in stripper outlet

As shown in Figure 11 and Figure 12, the model generally overpredicts both the loading and temperature of the lean solvent stream. As mentioned earlier, these discrepancies may be

reconciled with future modeling of the thermodynamics of the system and UQ of the properties models, hydraulic models, and mass transfer models.

3.3. Calculation of Delay Times for Liquid Samples during Dynamic Test Runs

When conducting dynamic test, it is important to note that measurements may have some time delay that may not be observed in steady-state test. If the measurements are not properly synced with the changes, the dynamic responses will not be observed correctly. For instance, in the specific case of measuring concentrations of the lean and rich loadings leaving the columns, the samples were transported, through piping, from the plant to the laboratory (where the MEA concentration and CO_2 loading are measured). Therefore, the time delay between the column and the laboratory needs to be calculated using hydraulic information.

The calculation was performed using the Fanning friction factor and the Darcy-Weisbach equation for the calculation of the average velocity, shown below.

$$f = 8\left(\left(\frac{8}{Re}\right)^{12} + (A+B)^{-1.5}\right)^{\frac{1}{12}} \tag{6}$$

$$\Delta p = f_D \frac{L}{D} \rho \frac{v^2}{2} \tag{7}$$

$$f_D = 4\, f \tag{8}$$

where A and B are given by the following relations

$$A = \left(2.457 \ln\left(\left(\left(\frac{7}{Re}\right)^{0.9} + 0.27\frac{\varepsilon}{D}\right)^{-1}\right)\right)^{16}$$

$$B = \left(\frac{37530}{Re}\right)^{16}$$

In these equations, f is the fanning friction factor, Re is the Reynolds number, ε is the roughness of the pipe, D is the pipe inner diameter, f_D is the Darcy friction factor, L is the length of the pipe, ρ is the liquid density and v the liquid velocity. As pressure drop (calculated from the sample take-off and return line pressures) and the length of the tubes were provided, through sensor data and isometric drawings of the pump inlet and outlet lines (for estimating the sample take-off and return line pressures), the delay time could be estimated. Typical delay times for the sampling of the lean and rich solvents were found to be 20.32 seconds and 20.87 seconds, respectively.

3.4. Future work

In order to complete model validation in both the steady-state and dynamic models using the valuable data collected by NCCC, some additional work on the model needs to be completed. Primarily, there is still work to be completed on the model and framework for uncertainty quantification of the VLE model, which is an important aspect of the properties models. A unified approach to development of deterministic mass transfer model and UQ of these models is being

developed. In addition, it is also necessary to complete work on the implementation of the dynamic model in gPROMS which is currently being delayed due to issues with the implementation of ASPEN properties in the gPROMS framework. Couple of issues must be considered while considering the dynamic data. Most of these are related to uncertainties in dynamic measurements. In addition to the holding tank, other issues that need data reconciliation include noisy measurements, nonworking sensors, and unmeasured make-up streams. Once the gPROMS model is working, then dynamic data reconciliation, will be completed and the dynamic model will be validated.